gebiology

Geobiology (2015) DOI: 10.1111/gbi.12140

Metabolic associations with archaea drive shifts in hydrogen isotope fractionation in sulfate-reducing bacterial lipids in cocultures and methane seeps

K. S. DAWSON,[1,2] M. R. OSBURN,[1,3] A. L. SESSIONS[1] AND V. J. ORPHAN[1]

[1]*Division of Geological and Planetary Science, California Institute of Technology, Pasadena, CA, USA*
[2]*Penn State Astrobiology Research Center, Pennsylvania State University, University Park, PA, USA*
[3]*Department of Earth and Planetary Sciences, Northwestern University, Evanston, IL, USA*

ABSTRACT

Correlation between hydrogen isotope fractionation in fatty acids and carbon metabolism in pure cultures of bacteria indicates the potential of biomarker D/H analysis as a tool for diagnosing carbon substrate usage in environmental samples. However, most environments, in particular anaerobic habitats, are built from metabolic networks of micro-organisms rather than a single organism. The effect of these networks on D/H of lipids has not been explored and may complicate the interpretation of these analyses. Syntrophy represents an extreme example of metabolic interdependence. Here, we analyzed the effect of metabolic interactions on the D/H biosignatures of sulfate-reducing bacteria (SRB) using both laboratory maintained cocultures of the methanogen *Methanosarcina acetivorans* and the SRB *Desulfococcus multivorans* in addition to environmental samples harboring uncultured syntrophic consortia of anaerobic methane-oxidizing archaea (ANME) and sulfate-reducing *Deltaproteobacteria* (SRB) recovered from deep-sea methane seeps. Consistent with previously reported trends, we observed a ~80‰ range in hydrogen isotope fractionation ($\varepsilon_{lipid-water}$) for *D. multivorans* grown under different carbon assimilation conditions, with more D-enriched values associated with heterotrophic growth. In contrast, for cocultures of *D. multivorans* with *M. acetivorans,* we observed a reduced range of $\varepsilon_{lipid-water}$ values (~36‰) across substrates with shifts of up to 61‰ compared to monocultures. Sediment cores from methane seep settings in Hydrate Ridge (offshore Oregon, USA) showed similar D-enrichment in diagnostic SRB fatty acids coinciding with peaks in ANME/SRB consortia concentration suggesting that metabolic associations are connected to the observed shifts in $\varepsilon_{lipid-water}$ values.

Received 4 November 2014; accepted 30 March 2015

Corresponding author: K. S. Dawson. Tel.: +1 (626) 395 6018; fax: +1 (626) 568 0935; e-mail: kdawson@caltech.edu; V.J. Orphan. Tel.: +1 (626) 395 1786; fax: +1 (626) 568 0935; e-mail: vjorphan@gps.caltech.edu

INTRODUCTION

Compound-specific D/H analysis of fatty acids provides information that may complement or independently constrain $\delta^{13}C$ data for understanding pathways of carbon assimilation (Sessions *et al.*, 1999; Valentine, 2009; Zhang *et al.*, 2009). For example, Zhang *et al.* (2009) found a ~500‰ range in D/H fractionation between lipids and water ($\varepsilon_{lipid-water}$) for pure cultures of *Proteobacteria* grown with different substrates, and the magnitude of fractionation was correlated to carbon metabolism. This led to the hypothesis that the isotopic composition of NAD(P)H reflects the catabolic pathway through which it is generated and thereby impacts the δD of lipids as a reductant during biosynthesis. The correlation of δD with carbon metabolism in bacterial cultures by extension indicates the potential for hydrogen isotopic analysis of bacterial lipids to distinguish between autotrophic and heterotrophic carbon metabolism by micro-organisms in the environment (Osburn *et al.*, 2011).

In environmental samples with complex microbial communities including hot springs (Naraoka *et al.*, 2010;

Osburn *et al.*, 2011), particulate organic matter (Jones *et al.*, 2008), and marine sediments (Li *et al.*, 2009) ranges for $\varepsilon_{lipid-water}$ measured were comparable to those observed in pure culture studies (Sessions *et al.*, 2002; Valentine *et al.*, 2004; Campbell *et al.*, 2009; Zhang *et al.*, 2009; Fang *et al.*, 2014; Heinzelmann *et al.*, 2015). Although similar ranges occur in both environmental and culture samples, the correlation of measurements from environmental samples with carbon metabolism may be complicated by the unknown influence of microbial metabolic interactions on δD. In an effort to better constrain, the potential impact of interspecies metabolic interactions on the resulting $\varepsilon_{lipid-water}$, we conducted a study using pure cultures, cocultures, and environmental samples.

The anaerobic oxidation of methane (AOM) in marine methane seeps is driven by methane-oxidizing archaea (ANME) in association with sulfate-reducing *Deltaproteobacteria* (SRB). Symbiotic micro-organisms, such as ANME/SRB consortia, provide a means for testing the impact of interconnected metabolisms on $\varepsilon_{lipid-water}$. The common marine methane seep representatives of this syntrophic association are members of the ANME-2 archaea which form highly organized multicellular aggregations with either a *Desulfosarcina/Desulfococcus* (DSS) or *Desulfobulbaceae* (DSB) partner (Boetius *et al.*, 2000; Orphan *et al.*, 2001; Pernthaler *et al.*, 2008; Schreiber *et al.*, 2010; Green-Saxena *et al.*, 2014). AOM is an energetically limited metabolism made thermodynamically feasible by the coupling of methane oxidation (ANME) to sulfate reduction (SRB) through the exchange of electrons (Hoehler *et al.*, 1994; Stams & Plugge, 2009) and potentially chemical species such as zero-valent sulfur (Milucka *et al.*, 2012) between archaeal and bacterial partners.

Methanogenic archaea and SRB, which formed the basis for initial hypotheses regarding AOM (Zehnder & Brock, 1980), also form syntrophic consortia (Stams & Plugge, 2009; Hillesland & Stahl, 2010). The interactions between methanogens and SRB range from competitive to mutualistic depending on the availability of electron donors and acceptors (Zinder, 1993; Raskin *et al.*, 1996; Stams & Plugge, 2009). SRB outcompete methanogens for electron donors such as H_2, formate, and acetate in the presence of sulfate (Zinder, 1993; Raskin *et al.*, 1996), while more mutualistic interactions occur in low sulfate conditions where fermenting SRB are coupled to hydrogenotrophic methanogens through the production and consumption of H_2 (Stams & Plugge, 2009; Hillesland & Stahl, 2010). Additionally, multispecies biofilm formation and structure have been connected to more balanced SRB/methanogen compositions in both high and low sulfate conditions likely due to the dynamics of sulfate and electron donor transport (Nielsen, 1987; Raskin *et al.*, 1996; Brileya *et al.*, 2014).

Unlike their methane-oxidizing counterparts, there are cultured representatives of SRB and methanogens that allow for experiments on both monoculture and cocultures. Here, we use the metabolically versatile SRB, *Desulfococcus multivorans*, to examine trends in $\varepsilon_{lipid-water}$ associated with several substrates. We hypothesized that the naturally occurring trends in δD values of fatty acids characteristic of SRB associated with ANME in methane seep sediments from Hydrate Ridge, Oregon would correspond to the $\varepsilon_{lipid-water}$ values of autotrophic *D. multivorans*. Complexity in the environmental data led us to further examine the effect of metabolic associations on $\varepsilon_{lipid-water}$ using cocultures of *D. multivorans* with the methanogenic archaeon *Methanosarcina acetivorans*.

MATERIALS AND METHODS

Culture strains and growth

D. multivorans (DSM 2059) was grown in both monoculture and coculture with *M. acetivorans* (DSM 2834) on 20 mM formate, benzoate, lactate, pyruvate, glucose, succinate, or acetate. Additionally, cocultures were grown on the methanogenic substrates methanol (125 mM) or trimethylamine (TMA) (40 mM). *D. multivorans* monoculture media contained (g L^{-1}): NaCl, 7.0; $NaHCO_3$, 3.0; $MgCl_2{\cdot}6H_2O$, 1.5; KCl, 0.5; NH_4Cl, 0.3; KH_2PO_4, 0.2; $CaCl_2{\cdot}2H_2O$, 0.15; cysteine-HCl, 0.25; and resazurin, 0.001. *D. multivorans* media was supplemented with the SL-10 trace elements (Widdel *et al.*, 1983) and DSM-141 vitamin solutions (Deutsche Sammlung von Mikroorganismen). Coculture and *M. acetivorans* media contained (g L^{-1}) the following: NaCl, 23.4; $MgSO_4{\cdot}7H_2O$, 9.44; $NaHCO_3$, 5.0; KCl, 0.8; NH_4Cl, 1.0; Na_2HPO_4, 0.6; $CaCl_2{\cdot}2H_2O$, 0.14; cysteine-HCl, 0.25; and resazurin, 0.001. Coculture media were supplemented with a Na_2SeO_3 solution (3 μg L^{-1}) and the vitamin and trace element solutions DSM-141. All cultures were grown in triplicate in 20-mL culture tubes containing 10 mL of media, an N_2:CO_2 (80:20) headspace, a pH of 7.6, sealed with butyl rubber stoppers, and reduced after sterilization with a sodium sulfide solution to a final concentration of 1 mM. All cultures were grown at 32 °C without shaking. Pure cultures of *D. multivorans* were maintained on lactate, and *M. acetivorans* was maintained on methanol. Cocultures were initially constructed by inoculating fresh media with both *D. multivorans* and *M. acetivorans* where lactate and methanol were provided as substrates. Both monoculture and cocultures were transferred and grown to stationary phase once on different substrates prior to inoculation of cultures for D/H experiments. Optical density (OD) at 600 nm was used to determine growth curves and to harvest cultures for D/H analysis during late exponential phase. Growth rates were calculated from OD_{600} values

as described by Widdel (2010). Exponential phase cultures were centrifuged for 10 min at 4500 × *g* yielding cell pellets ranging from 0.1 to 3.0 mg of dry mass. These were stored at −80 °C before extraction. Aliquots of exponential phase culture were fixed with paraformaldehyde for microscopy analysis according to Dawson *et al.* (2013).

Sample collection

Samples were collected from Hydrate Ridge, Oregon as part of the *R/V Atlantis* cruise 18–10 in September 2011. Using the *ROV Jason II*, sediment push cores were collected from several distinct seep environments characterized by the presence of chemosynthetic clam beds (PC23) or microbial mats (PC18, PC36, and PC47) as well as from nearby reference sites (PC3) characterized by the absence of seep microbial/macrofaunal communities at the sediment surface. Sediment push cores were processed shipboard in 3-cm intervals according to Orphan *et al.* (2001) and stored at −80 °C until lipid or DNA extraction.

PC3 (44°N 40.05 125°W 6.03) was collected as a reference core. Although no active methane seepage was detected, carbonate nodules below the 6-cm horizon point to low CH_4 flux or past AOM activity. PC47 (44°N 40.02 125°W 6.00) was collected through a white microbial mat. PC18 (44°N 40.02 125°W 7.51) was taken through a pink/white microbial mat within an area of active methane venting. PC36 (44°N 40.02 125°W 6.00) was taken through a yellow microbial mat and showed evidence of degassing during recovery resulting in large air pockets in the core. PC23 (44°N 40.19 125°W 5.88) was recovered from a chemosynthetic clam bed with live *Calyptogena* clams present in the 0- to 3-cm horizon and 3- to 6-cm horizons.

Lipid extraction and quantitation

Frozen cell pellets were lyophilized and pre-weighed prior to extraction. Lipid extraction and transesterification to fatty acid methyl esters (FAMEs) were performed simultaneously at room temperature with 1 mL hexane and 2 mL 0.5 N NaOH in anhydrous methanol. The reaction was neutralized after 10 min with 70 μL glacial acetic acid, and the FAMEs were subsequently extracted with 2 mL water and 2 mL hexane (Griffiths *et al.*, 2010). A solution of *n*-tricosane (40 ng μL^{-1}) was used as an internal standard for extraction efficiency and quantitation and was added prior to transesterification.

Frozen sediment samples were lyophilized prior to extraction. Lipid extraction followed the methods described by Li *et al.* (2009). Sediment samples were saponified with 0.5N NaOH in 4:1 methanol: water at 65 °C for 2 hours. The saponified material was subsequently acidified and extracted with methyl tert-butyl ether (MTBE) and a 5% NaCl solution. Extracts were concentrated under a stream of N_2 and then passed through a column packed with acid-washed Cu filings to remove S^0. Compound classes were next separated by solid-phase extraction (SPE) using 0.5 g of an aminopropyl stationary phase (Phenomenex, Torrance, CA, USA). Fractions were eluted as follows: F1, 5 mL hexane; F2, 8 mL 4:1 hexane: dichloromethane (DCM); F3, 10 mL 9:1 DCM: acetone; and F4, 10 mL 4% formic acid in DCM. F3, which contained alcohols including archaeol (AR) and hydroxyarchaeol (AR-OH), was reacted with acetic anhydride/pyridine to form acetyl ester derivatives. Fraction 4, which contained fatty acids, was derivatized with BF_3/methanol to form fatty acid methyl esters (FAMEs).

FAMEs were analyzed by gas chromatography–mass spectrometry (GC-MS) on a Thermo-Scientific Trace-DSQ with a ZB-5 ms column (30 m × 0.25 mm, 0.25 μm i.d.) using a PTV injector operated in splitless mode. The oven temperature program was 100 °C to 320 °C (held 20 min) at 6 °C min^{-1}. Acetyl esters, including archaeol and hydroxyarchaeol, were analyzed by GC-MS on a Thermo-Scientific Trace-ISQ with a ZB-5 ms column (30 m × 0.25 mm, 0.10 μm i.d.) using a PTV injector operated in splitless mode. The oven temperature program was 100 °C to 310 °C (held 1 min) at 15 °C min^{-1}, 310 °C to 330 °C at 2 °C min^{-1} (held 10 min). Archaeol was identified by comparison with an authentic standard of 1,2-di-O-phytanyl-*sn*-glycerol (Avanti Polar Lipids Inc., Alabaster, AL, USA). Quantitation was achieved using a flame ionization detector (FID) by comparing the integrated FID signals from sample peaks to a standard curve for a dilution series of 1,2-di-O-phytanyl-*sn*-glycerol. Peak areas were calculated using THERMO XCALIBUR software version 2.1. Compound identification was based on comparison of the mass spectra to the authentic standard and retention time.

Hydrogen isotope measurements

After centrifuging cultures to pellet cells, an aliquot of the supernatant was transferred to 2-mL glass vials and stored at −20 °C. Water D/H analysis was carried out on a Los Gatos DLT-100 Liquid–Water Isotope Analyzer. Samples were measured in tenfold replicate and then normalized to the VSMOW scale using a 2-point calibration against two standards (δD = −117.0‰ and −10.6‰) (Coplen *et al.*, 2006). Precision was ± 1.2‰ (n = 79; 1σ).

D/H ratios of FAMEs were measured using a Thermo-Finnigan Trace GC coupled to a Delta^{plus}XP isotope ratio mass spectrometer (IRMS) via a pyrolysis interface maintained at 1430 °C. An external standard comprising a mixture of eight FAMEs was analyzed every sixth sample. Samples were injected using a PTV injector operated in splitless mode onto a ZB-5 ms column (30 m, 0.25 mm i.d., 1.0 μm film) with a He carrier gas (1.4 mL min^{-1}). The GC oven temperature program was 100 °C (held

1 min) to 205 °C at 20 °C min^{-1} to 220 °C at 0.6 °C min^{-1} to 320 °C (held 8 min) at 20 °C min^{-1}. Peaks were identified by a comparison of relative retention time and magnitude to GC-MS chromatograms. Isotope ratios were calculated using ISODAT NT 2.0 software using methane reference gas peaks for calibration as previously described (Wang & Sessions, 2008). The H_3^+ factor was measured daily and ranged from 2.182 to 2.848 across all analyses (Sessions *et al.*, 2001). Isotopic compositions are reported in the conventional δD notation as permil (‰) deviations from the VSMOW standard. All data were corrected for the addition of methyl hydrogen during derivatization. The δD of methyl hydrogen was determined by the derivatization and analysis of phthalic acid with a known δD. The root-mean-squared error for the external FAME standard mixture averaged 4.0‰ (1.7–6.9‰, $n = 68$). The standard deviation for replicate analyses of culture samples averaged 7.5‰ ($n = 64$) and of environmental samples averaged 10.7‰ ($n = 295$). All samples were run in duplicate. Fractionation between lipids and culture water was calculated as $\varepsilon_{l\text{-}w} = (\alpha_{l\text{-}w} - 1)$, where $\alpha = [(\delta_l + 1)/(\delta_w + 1)]$ and are reported in ‰ as per Coplen (2011).

Aggregate counts and microscopy of sediments and cocultures

Sediment samples were fixed for microscopy immediately after push cores were sectioned in 3 cm increments by adding 4% paraformaldehyde (PFA) to sediment–seawater mixtures in a 1:1 ratio and incubating at 4 °C for 12 hours. Fixed samples were washed with 3× phosphate-buffered saline (PBS) and stored in 1:1 3× PBS: ethanol at −20 °C. Laboratory cultures were fixed with a 3:1 mixture of 4% PFA and 3× PBS after centrifuging to pellet 1 mL of culture. Fixed cultures were incubated for 3 hours at 4 °C and subsequently washed and stored in the same manner as sediment samples. Prior to microscopy in the sediment samples, a Percoll (Sigma-Aldrich, USA) density gradient was applied to concentrate cells and remove sediment particles. Briefly, 200 μL of well-mixed sediment slurry, 700 μL 1M TRIS-EDTA buffer pH 8, and 100 μL 100 mM sodium pyrophosphate were combined and heated at 60 °C for 3 min and then sonicated with an ultrasonication wand for 3 × 10s on ice. To the bottom of this mixture, 1 mL Percoll was added and then centrifuged at 12000 × *g* for 20 min. The band of cellular material that formed at the Percoll/buffer interface was collected and used for further microscopy.

Fluorescence *in situ* hybridization (FISH) was performed as described previously (Glöckner *et al.*, 1996), using nucleotide probes targeting archaea (Arc915) (Stahl & Amann, 1991), bacteria (EUB338mix) (Amann *et al.*, 1990), *Desulfococcus/Desulfosarcina* (DSS658) (Manz *et al.*, 1998), ANME-2c (ANME-2c-760) (Knittel *et al.*, 2005), and ANME (Eel_MsMx-932) (Boetius *et al.*, 2000). Oligonucleotide probes were labeled at the 5′ end with either a FAM or cy3 dye and used in a final concentration of 5 ng μL^{-1} for FISH experiments. Following hybridization, cells were stained with 4′,6-diamidino-2-phenylindole (DAPI) and mounted with Vectashield (Vectashield Laboratories, USA). Populations of *D. multivorans* and *M. acetivorans* were determined from counts of 1000–2000 DAPI-stained cells. Aggregate counts were performed as described by Glass *et al.* (2014).

Sediment DNA extraction, sequencing, and analysis

DNA was extracted from all depth horizons of PC18 using the MoBio Ultraclean soil kit (MO BIO Laboratories Inc., Carlsbad, CA, USA) following a previously published protocol (Goffredi *et al.*, 2008). The V6 to V8 region of the 16S rRNA gene was amplified using the primers 926F (5′-AAACTYAAAKGAATTGRCGG-3′) and 1392R (5′ACGGGCGGTGTGTRC-3′) (Matsuki *et al.*, 2002) following the method previously described (Soo *et al.*, 2014). Multiplex identifiers were incorporated in the 1392R primer. Amplicons were sequenced using the Roche 454 GS-FLX Titanium platform at the Australian Centre for Ecogenomics, University of Queensland (Brisbane, Australia). Sequence data were demultiplexed and processed using a modified version of the QIIME pipeline (Caporaso *et al.*, 2010). The modified pipeline included the following: USEARCH (Edgar, 2010) for filtering, chimera checking and operational taxonomic unit (OTU) identification; taxonomic assignment by comparison with the SILVA 111 reference database (Quast *et al.*, 2013). Prior to sample comparison, singletons were removed and all samples were randomly subsampled to equal depth.

RESULTS

Substrate dependent D/H fractionation in fatty acids of *Desulfococcus multivorans* in pure culture

The efficacy of $\varepsilon_{lipid\text{–}water}$ as a diagnostic proxy for central metabolic pathway in SRB was studied using *D. multivorans* grown on seven different carbon sources including formate, benzoate, lactate, pyruvate, glucose, acetate, and succinate. *D. multivorans* monoculture growth rates ranged from 0.38 day^{-1} for lactate to 0.15 day^{-1} for acetate and had an average growth rate of 0.21 ± 0.08 day^{-1} (Table 1). Under all growth conditions, *D. multivorans* produces four major fatty acids 12-methyl tetradecanoic acid (*ai*-$C_{15:0}$), hexadecanoic acid ($C_{16:0}$), 14-methyl hexadecanoic acid (*me*-$C_{16:0}$), and methylenehexadecanoic acid (*cy*-$C_{17:0}$), which represent on average 90% of total extractable fatty acids (Table 1 and Fig. S1). The abundance-weighted mean $\varepsilon_{lipid\text{–}water}$ value calculated for the four most

Table 1 Summary of culturing experiments with *Desulfococcus multivorans* and *D. multivorans/Methanosarcina acetivorans* showing the measured δD and concentrations of fatty, acids, growth rates, and population makeup with different substrates

		Fatty acid $\varepsilon_{lipid-water}$ ‰, 1σ, μg/mg dry cell pellet)												$\varepsilon_{lipid-water}$				
Organism – substrate	δD_{water}	*ai*$C_{15:0}$			$C_{16:0}$			*me*$C_{16:0}$			*cy*$C_{17:0}$			Wt. mean		% *D. multi*	% *M. acet*	Rate (d^{-1})
Desulfococcus multivorans																		
Formate	−62.7	−198.8	10.1	0.45	−219.4	33.5	0.28	−192.1	14.6	0.01	−183.4	18.8	0.06	−205.0	19.1	100.0	0.0	0.21
Benzoate	−71.9	−188.6	7.8	2.80	−188.3	4.4	1.42	−178.5	6.0	0.63	−182.8	7.7	0.78	−186.6	6.7	100.0	0.0	0.17
Pyruvate	−65.2	−171.4	1.4	0.60	−183.9	7.8	0.50	−138.7	1.0	0.08	−128.5	8.2	0.05	−172.4	4.3	100.0	0.0	0.20
Lactate	−71.3	−160.2	14.7	9.05	−165.6	8.6	3.67	−190.7	14.6	2.18	−163.4	1.1	0.76	−165.8	12.6	100.0	0.0	0.38
Acetate	−72.2	−152.4	13.2	0.19	−127.7	15.6	0.17	n.m.	n.m.	0.03	−102.0	46.5	0.04	−137.0	17.4	100.0	0.0	0.15
Glucose	−60.2	−103.5	30.8	0.07	−151.0	14.3	0.09	−113.4	47.3	0.01	n.m.	n.m.	0.01	−130.4	22.3	100.0	0.0	0.18
Succinate	−65.7	−113.1	22.5	0.06	−133.2	15.5	0.10	n.m.	n.m.	0.01	−128.8	31.6	0.02	−126.3	19.5	100.0	0.0	0.21
Desulfococcus multivorans + Methanosarcina acetivorans																		
Methanol	−84.3	−178.1	3.8	0.05	−181.3	7.4	0.10	n.m.	n.m.	0.00	−137.5	2.1	0.01	−180.2	9.2	24.7	75.3	0.92
TMA	−78.3	−141.9	n.m.	0.03	−171.5	n.m.	0.01	n.m.	n.m.	0.02	n.m.	n.m.	0.02	−151.6	n.m.	13.5	87.5	0.92
Formate	−84.3	−153.8	3.4	0.14	−143.2	1.7	0.23	n.m.	n.m.	0.00	n.m.	n.m.	0.03	−147.2	2.4	74.4	25.6	0.46
Benzoate	−81.7	−175.2	1.5	1.09	−161.5	7.0	1.34	−147.9	6.5	0.11	−152.0	8.7	0.22	−167.7	12.1	50.1	49.9	0.47
Pyruvate	−83.5	−147.1	3.4	3.20	−179.1	2.3	1.10	−133.2	1.0	1.91	−123.7	2.1	1.44	−143.9	2.4	93.7	6.3	0.53
Acetate	−87.0	−177.2	5.0	0.23	−185.3	1.7	0.53	−134.2	47.4	0.02	−158.2	8.2	0.13	−177.9	5.0	66.8	33.2	0.29
Methanosarcina acetivorans																		
Methanol	−84.3	n.d.	n.d.	0.00	n.d.	n.d.	0.00	n.d.	n.d.	0.00	n.d.	n.d.	0.00	n.d.	n.d.	0.0	100.0	0.98

Wt. mean – abundance-weighted mean of $\varepsilon_{lipid-water}$ for the 4 most abundant fatty acids, 1σ indicates that standard deviation of $\varepsilon_{lipid-water}$ measurements, n.d. – not detected, n.m. – not measurable.

abundant fatty acids had a range of 80‰ (117‰ 1σ inclusive). Within this 80‰ range, there are 4 groups of values corresponding to carbon substrates associated with distinct central metabolic pathways (Fig. 1 and Fig. 2): Wood–Ljungdal – formate, −205‰; benzoate metabolism – benzoate, −187‰; pyruvate metabolism – lactate, pyruvate, −170‰; TCA cycle – acetate, succinate, −132‰. A large standard deviation in the measurements from cultures grown on formate causes a partial overlap with the observed range for cultures grown on benzoate. Glucose grown cultures (−130‰) more closely resemble substrates associated with the TCA cycle than pyruvate metabolism.

D/H fractionation in fatty acids during coculture of *Desulfococcus multivorans* with *Methanosarcina acetivorans*

Cocultures of sulfate-reducing *D. multivorans* and methanogenic *M. acetivorans* were grown on six substrates (formate, benzoate, pyruvate, acetate, methanol, and TMA). Four of these substrates provide a direct comparison with monocultures of *D. multivorans* (formate, benzoate, pyruvate, and acetate). Acetate can be utilized by both *D. multivorans* and *M. acetivorans*, while the other substrates (e.g., benzoate and pyruvate) are exclusive to *D. multivorans* with conversion to metabolites that are subsequently utilized by *M. acetivorans*. Methanol and trimethylamine (TMA) utilization are exclusive to *M. acetivorans* with conversion to metabolites that are subsequently utilized by *D. multivorans* (Fig. 2). Both *D. multivorans* and *M. acetivorans* were detectable by microscopy and by the presence of characteristic fatty acids (*D. multivorans*) and a C_{30}-isoprenoid lipid (*M. acetivorans*) in solvent extracts of cocultures after growth on all six substrates. Additional indications of growth by both organisms in cocultures included a strong sulfide odor when cells were harvested (*D. multivorans*) and evidence of gas production from the generation of overpressure in the culture tubes and visible distension of the butyl rubber stoppers (*M. acetivorans*).

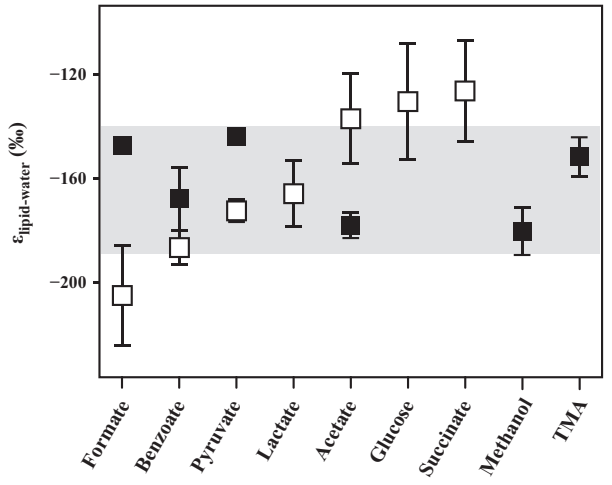

Fig. 1 Summary of D/H fractionation between fatty acids and water observed in culture experiments of *Desulfococcus multivorans* (open symbols) and cocultures of *D. multivorans* with *Methanosarcina acetivorans* (filled symbols) grown on a variety of substrates. $\varepsilon_{lipid-water}$ values are presented as the weighted mean of the four most abundant fatty acids (*ai*$C_{15:0}$, $C_{16:0}$, *me*$C_{16:0}$, *cy*C17:0). Error bars are ± 1 standard deviation. *D. multivorans* displayed an 80‰ range in $\varepsilon_{lipid-water}$ when grown on different carbon substrates including distinct values associated with growth on substrates associated with the TCA cycle (acetate, succinate), pyruvate metabolism (pyruvate, lactate), benzoate degradation (benzoate), and formate metabolism (formate). Cocultures of *D. multivorans* and *M. acetivorans* exhibited less variable $\varepsilon_{lipid-water}$ values across the range of substrates. The shaded area indicated the ~40‰ range of coculture $\varepsilon_{lipid-water}$.

Growth rates of both organisms in cocultures ranged from 0.92 day^{-1} with TMA or methanol to 0.29 day^{-1} with acetate (Table 1). These rates reflect the relative abundance of *D. multivorans* (average monoculture growth rate = 0.21 ± 0.08 day^{-1}) and *M. acetivorans* (average monoculture growth rates = 0.98 day^{-1}). Fluorescence *in situ* hybridization (FISH) analysis of coculture composition by the time of harvesting (7–17 days) revealed that the cocultures with higher growth rates were dominated by *M. acetivorans* (75.3–85.7% in methanol or TMA, respectively), while cocultures with lower growth rates had a higher proportion of *D. multivorans* relative to *M. acetivorans* (Table 1).

The same fatty acids (*ai*-$C_{15:0}$, $C_{16:0}$, *me*-$C_{16:0}$, and *cy*-$C_{17:0}$) described above for *D. multivorans* were the most abundant fatty acids in cocultures (Fig. S1) and were used to calculate the abundance-weighted mean $\varepsilon_{lipid-water}$ values. The cocultures exhibit a reduced range in the weighted mean $\varepsilon_{lipid-water}$, 36‰ (45‰ 1σ inclusive), compared to the ~80‰ range observed in the monoculture. Comparison of $\varepsilon_{lipid-water}$ for the same substrate between monoculture and cocultures revealed D-enrichment of up to 58‰ (formate, benzoate, and pyruvate) or D-depletion of 41‰ (acetate), with the abundance-weighted means from cocultures converging on an average $\varepsilon_{lipid-water}$ of −161 ± 15‰ (Fig. 1, Table 1).

Natural trends in D/H of SRB fatty acids from methane seep sediments

Sediment depth profiles (0–15 cm) were analyzed in 3-cm intervals from three characteristic methane seep habitats including sediments underlying sulfide-oxidizing microbial mats (PC18, 36, 47), chemosynthetic clam beds (PC23), and low methane flux sediment outside of visible signs of seepage (PC3). For all depth profiles, the δD values of all measurable fatty acids differed by as much as 176‰ within a single depth horizon (73.5–175.9‰, avg = 134.4 ± 27.5‰), but for any individual fatty acid structure typically varied by < 40‰ (31.9 ± 9.4‰, n = 131)

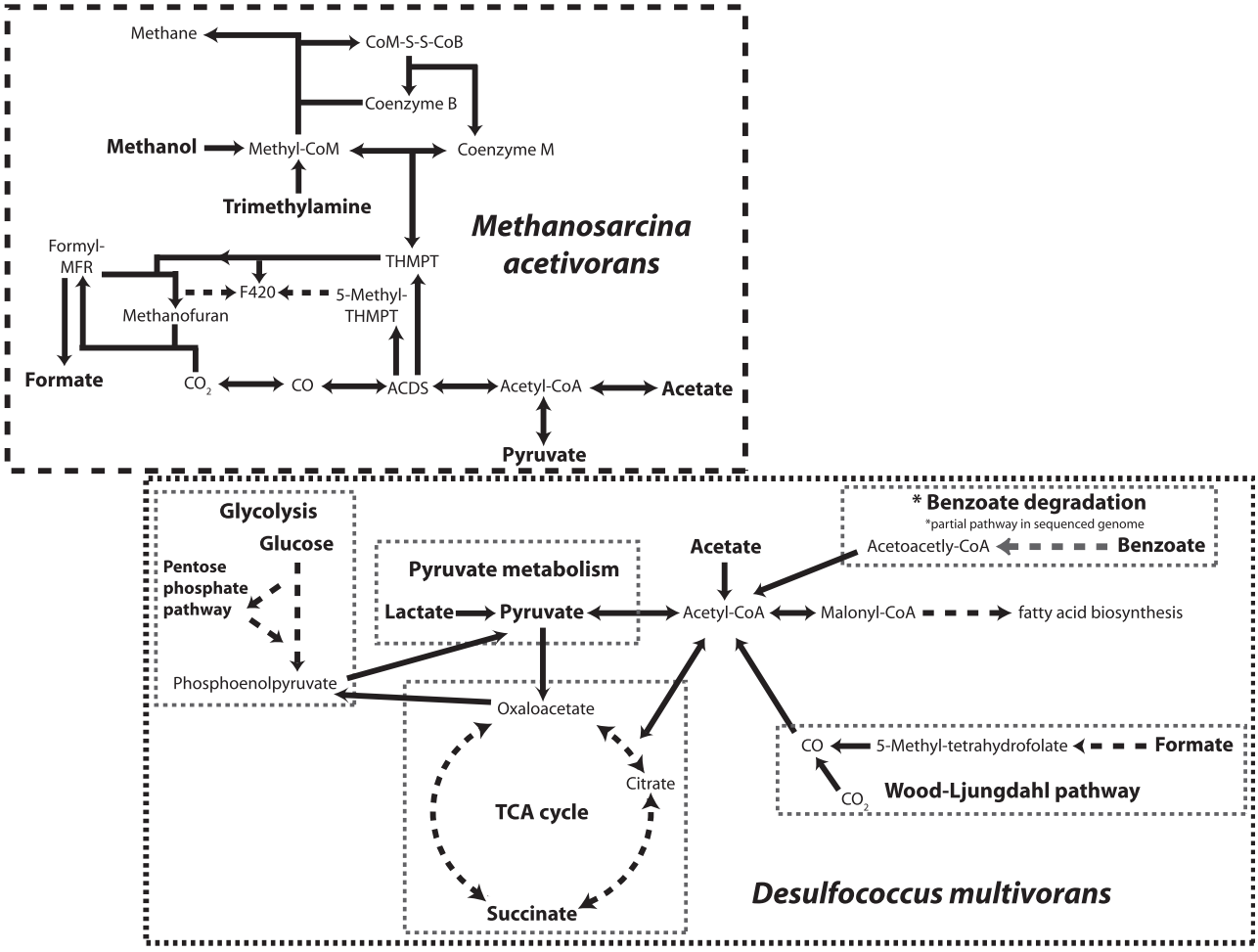

Fig. 2 Map of the central pathways for carbon metabolism in *Desulfococcus multivorans* and *Methanosarcina acetivorans* showing the potential connections between various pathways. The substrates used in these experiments are identified in bold. Dashed arrows indicate additional steps are present between the displayed compounds.CoM – coenzyme M; CoB – coenzyme B; MFR – methanofuran; THMPT – tetrahydromethanopterin; F420 – coenzyme F420; ACDS – acetyl-CoA decarbonylase/synthase complex; CoA – coenzyme A.

across all depths (Table 2). This variability between different fatty acids is likely due to the diversity of microorganisms contributing to the sedimentary lipid pool, either by *in situ* production or by deposition from pelagic environments.

Although multiple sources of fatty acids are present across the sampled depth profiles, a weighted mean $\delta D_{fatty\ acids}$ was calculated from all measureable fatty acids at each depth interval to examine whether they might reflect bulk metabolic trends within different seep habitats (Table 2). There was no significant difference in the weighted mean $\delta D_{fatty\ acids}$ between microbial mats and clam beds ($P = 0.5396$). However, the weighted mean $\delta D_{fatty\ acids}$ for low methane flux sediment resulted in more positive values and was significantly different than both the microbial mat ($P = 0.0005$) and the clam bed sediments ($P = 0.0039$). All of the depth profiles show an increase in the weighted mean $\delta D_{fatty\ acids}$ that is not significantly correlated with the concentration of sulfide ($r = 0.4018$, $P = 0.0761$) or sulfate ($r = -0.3770$, $P = 0.0710$), but is significantly correlated with ANME-2/DSS aggregate abundance ($r = -0.7382$, $P = 5.8 \times 10^{-5}$).

A subset of the fatty acids including several proposed as diagnostic biomarkers for AOM associated SRB (*i*-$C_{15:0}$, *ai*-$C_{15:0}$, $C_{16:1\ \omega5,6}$, *cy*-$C_{17:0}$) (Elvert *et al.*, 2003; Niemann & Elvert, 2008) displayed greater variation in δD across the depth profile. In particular, *cy*-C_{17-0}, which was also present in *D. multivorans* had a 50–90‰ range in measured δD with more D-enriched values corresponding to depths with higher concentrations of ANME-2/DSS aggregates and AR-OH (Fig. 3, Fig. 4 and Table 2). Exceptions to the association of D-enrichment with aggregate concentration include the top depth horizon of several cores, as well as PC36, which was disrupted by degassing

Table 2 Summary of Hydrate Ridge geochemistry for PC3, PC18, PC23, PC36, and PC47 showing concentrations and δD_{lipid} for *ai*-$C_{15:0}$ and *cy*-$C_{17:0}$ fatty acids, characteristic of sulfate-reducing bacteria, aggregate concentrations, archaeaol (AR) and hydroxyarchaeol (AR-OH) concentrations, and $\delta^{13}C_{AR\text{-}OH}$

Push core	Description	Avg. Depth (cm)	Fatty acid (δD ‰, 1σ, ug/g dry sediment)									Aggregates ($mL^{-1} \times 10^7$)	AR(μg/g)	AR-OH(μg/g)	AR-OH ($\delta^{13}C$ ‰)	$SO4^2$ (mM)	HS^- (mM)
			ai$C_{15:0}$			*cy*$C_{17:0}$			Wt. mean								
PC 3	Low	0	−127.4	0.9	0.77	−166.9	87.7	0.05	−123.0	15.9	8.54	n.d.	0.31	0.08	n.m.	23.99	0.00
	methane	3	n.m.	n.m.	0.00	n.m.	n.m.	0.00	n.m.	n.m.	0.02	n.d.	0.00	0.00	n.m.	18.99	0.00
	flux	6	n.m.	n.m.	0.03	n.m.	n.m.	0.01	−152.1	44.9	0.82	n.d.	0.00	0.00	n.m.	19.21	0.00
		9	−142.1	3.1	0.15	n.m.	n.m.	0.02	−129.4	8.8	2.08	n.d.	0.32	0.14	n.m.	22.01	0.10
		12	−151.1	6.6	0.25	n.m.	n.m.	0.02	−136.3	6.2	2.78	n.d.	0.38	0.09	n.m.	10.21	0.00
PC 18	Microbial mat	0	−187.2	1.2	0.39	−151.8	12.5	0.11	−205.3	6.5	26.73	25.88	1.45	0.32	−75.7	8.06	5.92
		3	−165.2	2.8	0.14	−174.5	5.3	0.06	−205.2	6.0	3.95	32.25	1.28	0.42	−88.6	1.22	18.37
		6	−147.6	7.0	0.17	−195.5	1.8	0.08	−210.2	7.2	10.49	32.63	0.88	0.21	−90.7	0.22	19.94
		9	−172.0	0.6	1.40	−239.8	4.8	0.64	−224.3	4.2	21.09	23.63	0.26	0.01	−108.6	0.45	24.63
		12	−174.7	2.1	1.80	−247.4	2.3	0.78	−220.3	4.3	26.1	12.38	1.16	0.06	n.m.	0.02	24.71
PC 23	Clam bed	0	−202.6	0.5	1.60	−240.3	1.5	0.16	−208.7	6.3	55.21	1.13	0.00	0.00	n.m.	16.64	0.09
		3	−199.5	19.2	0.21	−141.3	8.1	0.05	−190.8	18.6	4.93	2.25	0.06	0.00	−71.8	20.40	0.83
		6	−163.9	13.8	0.18	−131.8	0.2	0.03	−198.4	4.8	3.72	0.75	0.03	0.00	n.m.	17.03	0.00
		9	n.m.	n.m.	0.03	n.m.	n.m.	0.04	−162.1	2.2	2.97	0.38	0.00	0.00	n.m.	10.68	0.55
		12	n.m.	n.m.	0.01	n.m.	n.m.	0.00	−164.8	n.m.	0.87	0.00	0.01	0.00	n.m.	n.m.	n.m.
PC 36	Microbial mat	0	−198.9	0.7	1.84	−215.3	1.7	0.95	−239.3	4.0	74.54	12.56	0.21	0.01	−114.9	11.30	2.34
		3	−185.5	n.m.	1.22	−162.4	n.m.	0.88	−217.1	n.m.	16.99	10.13	0.00	0.00	n.m.	0.00	12.73
		6	−153.9	0.9	0.31	−178.6	31.3	0.09	−192.8	11.6	7.45	11.63	0.00	0.00	−101.0	0.47	12.44
		9	n.m.	n.m.	0.08	n.m.	n.m.	0.08	−179.1	5.0	4.22	2.25	0.00	0.00	n.m.	5.63	4.66
PC 47	Microbial mat	0	−165.9	13.9	15.65	−201.9	5.9	0.97	−185.7	17.9	159.85	2.40	3.69	0.08	−118.0	19.81	1.81
		3	−150.9	20.7	2.32	−138.9	23.2	0.19	−177.7	15.9	23.86	1.70	0.07	0.01	n.m.	12.34	5.89
		6	−167.2	12.2	2.00	−148.4	16.9	0.35	−179.5	10.1	15.56	4.80	1.50	0.37	−111.4	15.86	4.01
		9	−174.8	2.4	0.31	−194.1	1.1	0.01	−137.4	8.8	1.98	1.10	0.07	0.02	n.m.	9.85	12.58
		12	−176.2	30.9	0.19	n.m.	n.m.	0.01	−127.7	27.4	1.4	1.40	0.00	0.00	n.m.	1.25	17.21

1σ indicates that standard deviation of δD measurements, Wt. mean – abundance-weighted mean of $\delta D_{fatty\ acids}$ for all fatty acids reported in Table S1, n.d. – not detected, n.m. – not measurable.

during retrieval resulting in mixing between depth horizons.

To compare the isotopic compositions with 16S rRNA-based archaeal and bacterial diversity, DNA was extracted from 5 depth horizons in one of the microbial mat sediment samples (PC18) and sequenced by tag pyrosequencing on a Roche 454 GS-FLX Titanium platform. After quality control filtering, the number of sequences per depth was as follows: 0–3 cm – 1181; 3–6 cm – 1113; 6–9 cm – 5463; 6–9 cm – 6710; 9–12 cm – 6710; and 12–15 cm – 8002. Sample comparisons were carried out following the removal of singletons and random subsampling to an even depth of 1113 sequences. A heat map and table of the genera representing > 1% of sequences for each depth horizon showed a peak in ANME-2 abundance at the 3- to 6-cm depth horizon (Fig. 5, Table S1). The Seep-SRB1 group of *Deltaproteobacteria*, which represents a subclade within the DSS and is thought to be the dominant bacterial lineage that associates with ANME-2 (Schreiber *et al.*, 2010), was consistently the most abundant bacterial genus detected below the 0- to 3-cm horizon. Percentages of ANME groups relative to all archaeal sequences and DSS and DSB relative to all bacteria show peaks in both the ANME 2c and DSS sequence abundance that correspond with peaks in cell aggregate counts as well as the concentration of hydroxyarchaeol (AR-OH) and the seep SRB biomarker *cy*-$C_{17:0}$ (Fig. 3 and Fig. 4).

DISCUSSION

Correlation with carbon metabolism in SRB

Desulfococcus multivorans is a metabolically versatile SRB with central carbon metabolic pathways that include the Wood–Ljungdahl pathway, benzoate degradation, pyruvate metabolism, a modified glycolysis pathway, and the TCA cycle (Brown *et al.*, 2013) (Fig. 1 and Fig. 2). Differences in the central metabolic pathway of *D. multivorans* correlate to ranges in $\varepsilon_{lipid-water}$ values (Fig. 1). However, the extent of variability occurs on a smaller scale than the 500‰ range reported by Zhang *et al.* (2009). The smaller and more D-depleted range of fractionation for *D. multivorans* is consistent with other described SRB such as *Desulfobacterium autotrophicum* (Campbell *et al.*, 2009) and *Desulfobacter hydrogenophilus* (Osburn, 2013), as well as for sulfur-oxidizing bacteria (Naraoka *et al.*, 2010; Heinzelmann *et al.*, In review). While $\varepsilon_{lipid-water}$ for autotrophic growth conditions in these three SRB overlap with previously shown ranges for photoautotrophy and chemoautotrophy (Valentine, 2009; Zhang *et al.*, 2009), these obligate anaerobes show more negative values for heterotrophic growth conditions compared to their aerobic and facultatively anaerobic counterparts (Fig. 6).

The differences in $\varepsilon_{lipid-water}$ (Fig. 6) are likely due to the physiology of SRB and may include slower growth rates allowing greater equilibration between NAD(P)H and cellular water (Kreuzer-Martin *et al.*, 2006). Specific growth rate-dependent effects on D/H fractionation between intracellular and extracellular water have been documented in the aerobic heterotroph *Escherichia coli*, where in exponentially growing cultures, a greater proportion of intracellular water was isotopically distinct from the extracellular water as compared to those in stationary phase (53% vs. 23%) (Kreuzer-Martin *et al.*, 2006).The difference observed in their experiments was due to the contribution of water generated from metabolic reactions. However, in our studies, the difference between growth rates for pure cultures of *D. multivorans* on the various substrates was small ($0.15–0.38\ day^{-1}$, avg = $0.21 \pm 0.08\ day^{-1}$) and not correlated with $\varepsilon_{lipid-water}$, making growth rate alone an unlikely source for the variation observed for the seven utilized substrates. Kreuzer-Martin *et al.* (2006) also noted that the δD values of metabolic water in stationary-phase cultures were ~90‰ more negative than in exponentially growing cultures, which was suggested to be a result of reduced proton pumping. The slower exponential growth rate of *D. multivorans* and other SRB relative to *E. coli* could similarly result in D-depleted metabolic water and explain the more negative $\varepsilon_{lipid-water}$ measured in this experiment as compared to aerobic heterotrophs grown on the same substrates (Zhang *et al.*, 2009).

Influence of microbial interactions

In contrast to the SRB monocultures, $\varepsilon_{lipid-water}$ values for cocultures of *D. multivorans* and *M. acetivorans* grown on different substrates did not correlate with metabolic pathway (Fig. 1) or distinguish between autotrophic (formate) versus heterotrophic (benzoate, pyruvate, and acetate) metabolism (Fig. 6). Rather, D/H fractionation was surprisingly consistent across all incubation conditions and with differing proportions of the two species in culture (*D. multivorans* vs. *M. acetivorans* dominant). Changes in $\varepsilon_{lipid-water}$ were particularly unexpected during coculture growth on substrates exclusively utilized by *D. multivorans* (formate, benzoate, and pyruvate) since these must be metabolized through the same pathways as the monoculture. While the mechanism is not fully understood at this time, here, we consider three possibilities which may have contributed to shifts in $\varepsilon_{lipid-water}$ during coculture growth.

One possible explanation for the difference in $\varepsilon_{lipid-water}$ between monoculture and coculture could be that *D. multivorans* did not directly metabolize the provided carbon source when grown with *M. acetivorans*. For example, SRB, including *D. multivorans*, produce polyhydroxyalkanoate (PHA) granules for carbon storage (Hai *et al.*, 2004), which could represent a common carbon source in

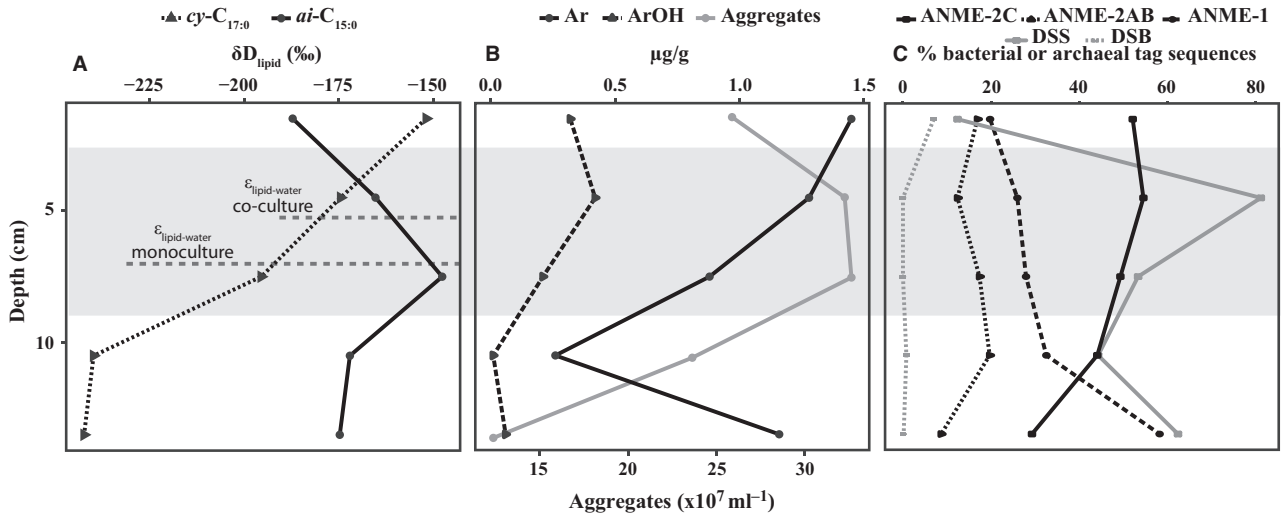

Fig. 3 Comparison of δD_{lipid} for the fatty acids *ai*C_{15} and *cy*C_{17} in PC 18 (A), concentrations of archaeol (Ar), hydroxyarchaeol (ArOH), and aggregate counts. The dashed lines indicate the range of weighted mean $\varepsilon_{lipid-water}$ values for *D. multivorans* (−208 ± 23‰ to −117 ± 18‰) and the *D. multivorans*/*M. acetivorans* coculture (−165 ± 15‰). (B) 16S rRNA tag pyrosequencing data (C) for a microbial mat core from Hydrate Ridge North. The shaded region contains the greatest abundance of sequences associated with ANME-2c/DSS aggregates, the highest aggregate counts, high concentration of archaeal biomarkers, and shifts to more enriched D/H values for two sulfate-reducing bacterial fatty acid biomarkers.

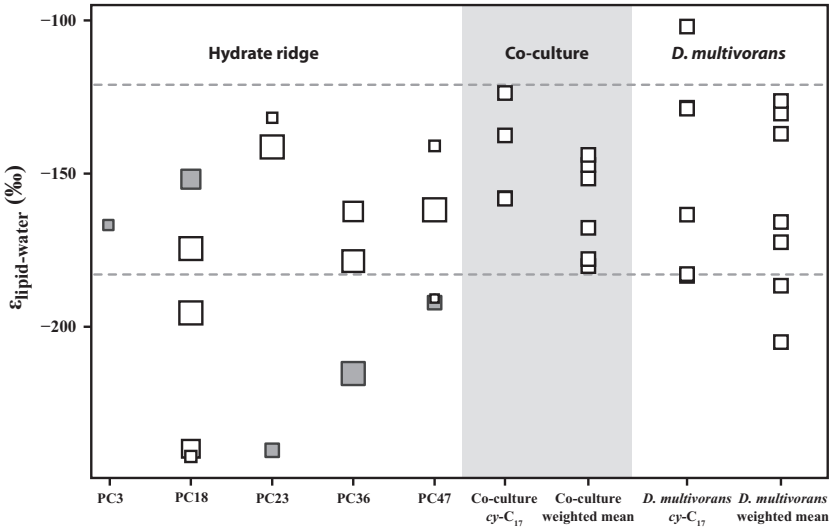

Fig. 4 $\varepsilon_{lipid-water}$ of *cy*-$C_{17:0}$ fatty acid, characteristic of sulfate-reducing bacteria (DSS) associated with ANME-2, extracted from methane seep sediment push cores within sulfide-oxidizing microbial mats (PC18, 36, 47), a chemosynthetic clam bed (PC23) and a low methane flux site (PC3). The size of the squares correlates to the abundance of the ANME/SRB aggregates at the same depth interval. Samples with a greater abundance of ANME/SRB aggregates correspond to more D-enriched *cy*-$C_{17:0}$. Most aggregate containing samples have δD-*cy*-$C_{17:0}$ within the same range observed for cocultures of *Desulfococcus multivorans* and *Methanosarcina acetivorans* (dashed lines). The more D-depleted core top samples (filled squares) of PC23, PC36, and PC47 may reflect a greater contribution from organisms within microbial mats. $\varepsilon_{lipid-water}$ for *cy*-$C_{17:0}$ and the weighted mean for the coculture (shaded region) and *D. multivorans* are shown for comparison.

all coculture conditions. Catabolic breakdown of carbon storage granules and production of both acetyl-CoA and NAD(P)H by the associated pathway could partially explain the convergence to a common $\varepsilon_{lipid-water}$. A correlation between D-enrichment and utilization of internal carbohydrate stores has previously been reported in plant lipids (Sessions, 2006). The intracellular PHA pool has been shown to be in constant flux (Taidi *et al.*, 1995) with net degradation promoted by the absence of an external carbon source (Jendrossek & Handrick, 2002). Differential flux of PHA between monocultures and cocultures might occur due to PHA degradation in carbon-limited

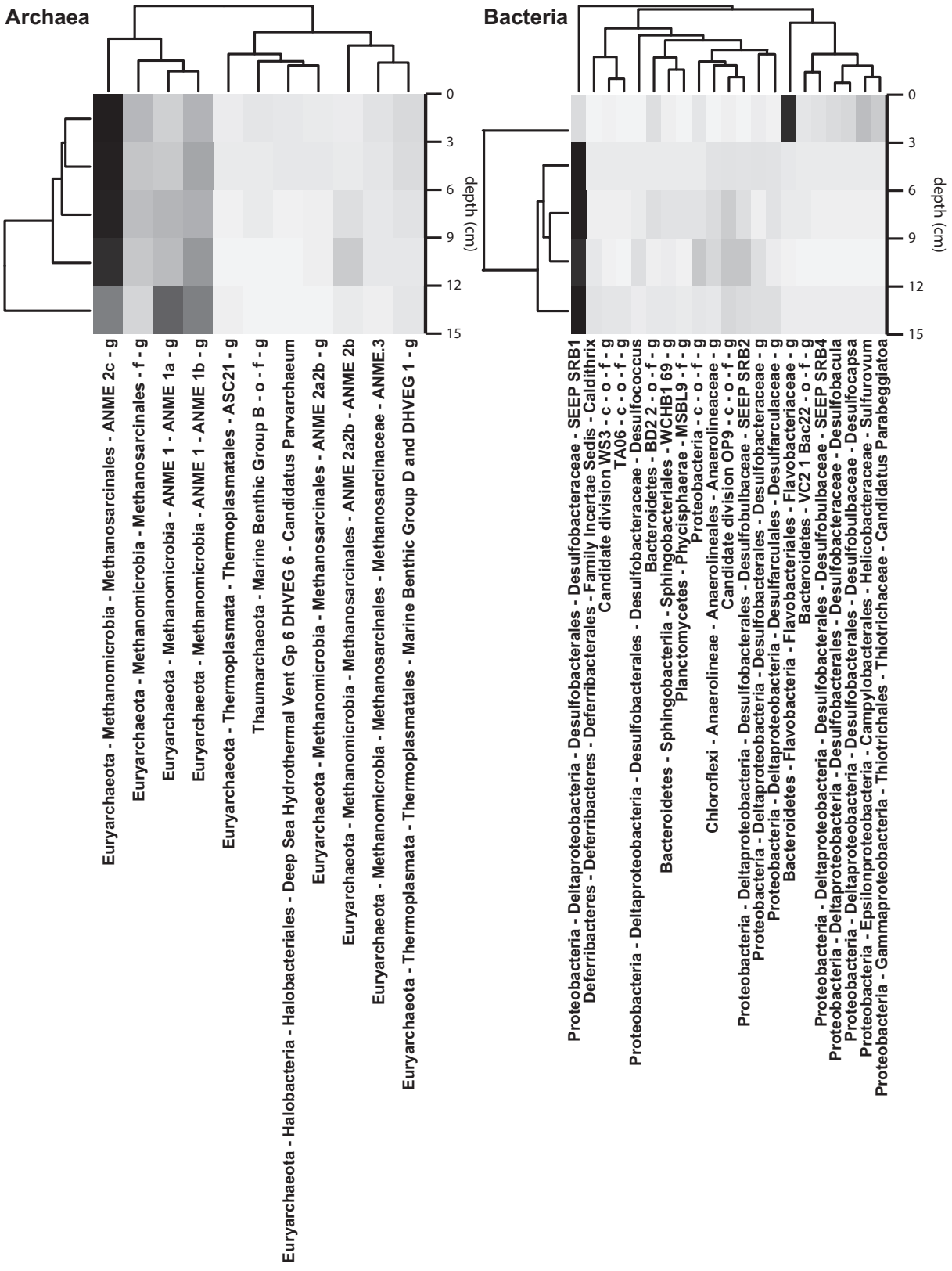

Fig. 5 Heat maps of archaeal and bacterial 16S rRNA tag pyrosequencing results showing genera representing more than 1% of at least one depth horizon from sediments underlying a sulfide-oxidizing microbial mat (PC18). The most abundant archaeal taxa is ANME-2c, and the most abundant bacterial taxa is the Seep-SRB1 group of *Deltaproteobacteria*.

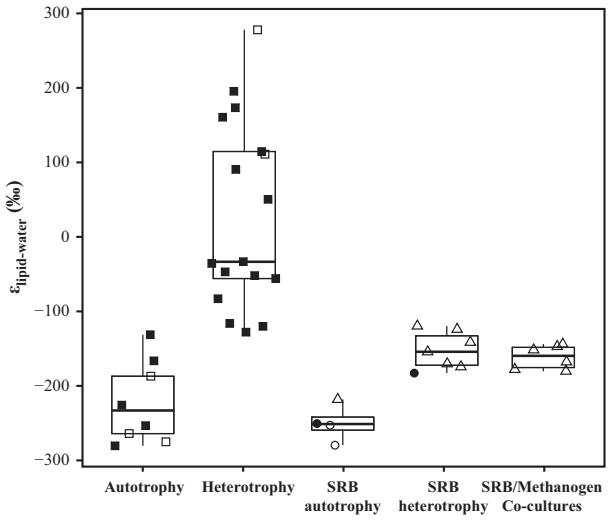

Fig. 6 Box plot comparison of D/H fractionation between fatty acids and water reported for 8 species of *Proteobacteria* (filled squares) (Zhang *et al.*, 2009) (open squares) (Heinzelmann *et al.*, In review) to the D/H fractionation of the SRB including *Desulfococcus multivorans* (triangles) (this study), *Desulfobacter hydrogenophilus* (filled circles) (Osburn, 2013), and *Desulfobacterium autotrophicum* (open circles) (Campbell *et al.*, 2009). Autotrophic and heterotrophic growth conditions are shown in separately. Autotrophic growth is distinguished from heterotrophic growth by lower D/H ratios (larger fractionations). The three different SRB examined to date exhibited a smaller range and a more D-depleted mean as compared to the aerobic *Proteobacteria* in the Zhang *et al.* (2009). Cocultures of *D. multivorans* and methanogenic archaeon *M. acetivorans* resulted in the smallest range of fractionation and no observable differentiation between autotrophy (formate) and heterotrophy (benzoate, pyruvate, acetate, methanol, and TMA) across the six substrates tested.

conditions during growth on competitive substrates (acetate) or on substrates exclusive to *M. acetivorans* (methanol, TMA). However, this cannot explain the results from growth on substrates exclusive to *D. multivorans* (formate, benzoate, and pyruvate). Additionally, cocultures were propagated multiple times under the experimental conditions prior to collection and lipid analysis making it unlikely that the observed growth could be due solely to residual PHA granule utilization.

A second possible explanation is that the measured $\varepsilon_{lipid\text{–}water}$ values for *D. multivorans* in coculture could be the result of mixotrophic growth on provided and excreted substrates. Metabolic by-products from *M.* acetivorans may represent another source of substrates used by *D. multivorans* in the coculture. *M. acetivorans* has been reported to be capable of excreting organic acids such as acetate or formate (Rother & Metcalf, 2004) or methyl sulfides (Moran *et al.*, 2008; Oelgeschläger & Rother, 2009). *D. multivorans* growth on formate resulted in the most D-depleted measurements of $\varepsilon_{lipid\text{–}water}$, while growth on acetate resulted in among the most D-enriched values (Fig. 1). Cocultures converged on an average $\varepsilon_{lipid\text{–}water}$ of $-165 \pm 15‰$, which is approximately the mean of acetate and formate growth ($-168‰$). While acetate or formate generated as a by-product of coculture growth will likely have a different H isotopic composition than the substrate solutions used in culturing experiments, the NAD(P)H generated through by-product metabolism should have an isotopic composition reflective of the catabolic pathway. Moreover, substrates (including acetate) are expected to contribute at most 25% of lipid hydrogen (see below). Thus, mixotrophic growth on the provided substrate and excreted acetate or formate could conceivably result in the muted range of $\varepsilon_{lipid\text{–}water}$ values measured in the *D. multivorans* and *M. acetivorans* cocultures.

Finally, changes in $\varepsilon_{lipid\text{–}water}$ between monoculture and coculture might indicate an additional source of hydrogen contributing to lipid biosynthesis. Several studies using D-labeled tracers have determined the sources of hydrogen in fatty acids to be NAD(P)H (~50%), acetyl-CoA (~25%) and water (~25%) (Seyama *et al.*, 1978; Saito *et al.*, 1980; Robins *et al.*, 2003). An important feature of syntrophic methanogenic communities is interspecies electron transfer, the shuttling of reduced chemical species, particularly through the transfer of molecular hydrogen and formate (Stams & Plugge, 2009). Enzymes potentially involved in electron transfer, including NADH-linked dehydrogenases, NAD(P) transhydrogenases, and ferredoxin-NADP(+) reductases, have been observed in the genomes of syntrophic SRB (Sieber *et al.*, 2012) and are present in a partial genome of *D. multivorans* (Brown *et al.*, 2013). NAD(P) transhydrogenases, which catalyze the transfer of reducing equivalents between NADPH and NADH, were previously discussed by Zhang *et al.* (2009) as a means to D-enrichment of the NADPH pool in cases of high TCA cycle flux (Sauer *et al.*, 2004). While excess NADPH production from the TCA cycle seems improbable in the slow growing *D. multivorans,* the coupling of NAD(P) transhydrogenase and ferredoxin-NADP(+) reductase in other SRB (*Desulfovibrio alaskensis* G20, *Desulfovibrio vulgaris* Hildenborough) has been proposed as a means of energy conservation (Pereira *et al.*, 2011). NAD(P)H formed as a result of interspecies hydrogen transfer could provide an explanation for the observed convergence in $\varepsilon_{lipid\text{–}water}$ measured for cocultures.

We observed shifts in $\varepsilon_{lipid\text{–}water}$ values between monoculture and coculture growth of *D. multivorans* on the same substrates combined with the convergence of these values. These observations indicate a change in the hydrogen sources for fatty acid synthesis which could include the use of an alternative carbon source (storage granules, metabolic by-products) and NAD(P)H production via alternative metabolic pathways or an additional source of hydrogen related to the association of the methanogen and SRB. The mechanism needs to be examined in future studies; however, the experimental observation that the same organism grown on the same substrates can exhibit

significant differences in D/H ratio depending on whether it is grown alone or in coculture has implications for interpretation of these signals in the environment, especially in ecosystems supporting syntrophic associations (e.g., AOM described below).

Trends in sediment samples

While shifts in the abundance of various ANME groups are seen by microscopy (all cores) and 16S rDNA tag pyrosequencing (PC18), the composition of the SRB community (PC18) appears to remain consistent with depth (Fig. 3 and Fig. 5). Although, the SRB species composition does not vary with depth, peaks in the concentration of diagnostic biomarkers (*i*-$C_{15:0}$, *ai*-$C_{15:0}$, *cy*-$C_{17:0}$) indicate changes in the relative abundance of SRB to other bacteria (Fig. 5 and Table S2). This suggests that the observed trends in δD of methane seep SRB biomarkers may be associated with either depth related changes in substrate utilization or with bacterial–archaeal associations rather than shifts in the bacterial community.

To address the influence of either substrates or association of SRB with ANME archaea, we focus on the diagnostic biomarkers *ai*-$C_{15:0}$ and *cy*-$C_{17:0}$, which are present in both sediment and culture conditions. Based upon previously reported carbon and hydrogen isotope data (Wegener *et al.*, 2008; Kellermann *et al.*, 2012), we hypothesized that the D/H ratios of diagnostic AOM SRB biomarkers (e.g., *cy*-$C_{17:0}$) would reflect chemoautotrophic growth. However, while some of the δD values measured for both *cy*-$C_{17:0}$ and *ai*-$C_{15:0}$ correlate to ranges observed in autotrophic SRB pure cultures, the majority of values are consistent with what had been previously observed in pure culture heterotrophs and notably the values measured in our *D. multivorans* and *M. acetivorans* cocultures (Fig. 4 and Fig. 6). The more D-enriched δD values occur at the depths with higher concentrations of aggregates, while D-depleted δD values are associated with lower aggregate concentrations (Fig. 3 and Fig. 4). The correlation between aggregate concentration and D-enrichment suggests that a similar mechanism for shifting $\varepsilon_{lipid-water}$ may be occurring in both the methanogenic/sulfate-reducing cocultures as well as the *cy*-$C_{17:0}$-producing SRB partner of ANME archaea in the environmental methane seep.

In addition to methanogenesis rather than methanotrophy occurring, there were distinct differences between growth conditions of the cultures and environmental samples. The *D. multivorans* and *D. multivorans/M. acetivorans* cocultures were grown at temperatures and substrate concentrations intended to optimize growth, while the environmental conditions were both lower in temperature and substrate availability. The methanol and TMA coculture conditions may be most comparable to environmental conditions for SRB. In these conditions, the availability of substrates was limited to potential excreted byproducts of methanogen metabolism. However, $\varepsilon_{lipid-water}$ in the methanol and TMA cocultures was comparable to other cocultures with much higher substrate concentrations (Fig. 1). In the coculture, growth on excreted substrates or the generation of additional NAD(P)H reducing intermediates during interspecies electron transfer, are the more likely hypotheses for the observed $\varepsilon_{lipid-water}$ convergence. Both hypotheses are applicable to the AOM system where the metabolism of the ANME/SRB consortia involves the interspecies transfer of electrons and potential intermediates such as acetate, hydrogen and formate (Zehnder & Brock, 1980; Strous & Jetten, 2004; Orcutt & Meile, 2008).

Implications for the interpretation of fatty acid D/H in environmental samples

Microbial communities form interconnected biogeochemical networks which influence the geochemistry of natural systems. Although isolates of certain micro-organisms can be investigated in the laboratory, organisms rarely grow alone in the environment. While $\varepsilon_{lipid-water}$ values for pure cultures correlate with the central metabolic pathway of individual bacteria (Zhang *et al.*, 2009) and archaea (Dirghangi & Pagani, 2013), this did not hold true in cocultures of a SRB and a methanogen. Additionally, the δD values of *cy*-$C_{17:0}$ in sediment depth horizons containing high ANME-2/DSS aggregate abundance corresponds to the same $\varepsilon_{lipid-water}$ value ranges for the methanogenic coculture analogues (Fig. 3 and Fig. 4). Methanogenic degradation of organic matter often involves a community of bacteria that produce substrates for the final step of methane formation by archaea (Stams, 1994; Thauer, 1998; Kotsyurbenko, 2005; Strąpoć *et al.*, 2011) and anaerobic methanotrophy likewise relies on the coupling of multiple organisms (Hoehler *et al.*, 1994; Boetius *et al.*, 2000; Orphan *et al.*, 2001; Knittel *et al.*, 2005). The syntrophic nature and close association of cells in these communities, which favors interspecies electron transfer (Stams & Plugge, 2009) may explain the results of our coculture and environmental studies as well as complicate the assessment of autotrophy and heterotrophy based on D/H in some environments.

ACKNOWLEDGMENTS

We thank the shipboard, scientific crew and pilots of the R/V Atlantis and DSV Jason. Stephanie Connon, Fenfang Wu, and Lichun Zhang provided technical assistance. Laurence Bird and Katherine Freeman provided the $^{13}C_{lipid}$ measurements. We would also like to thank four anonymous reviewers for their comments toward improving this manuscript. This study was supported by a grant from the

Penn State Astrobiology Research Centre (through the NASA Astrobiology Institute (NNA09DA76A)) to VJO, a PSARC post-doctoral fellowship to KSD and an NSF Graduate Fellowship to MRO. Additional support was provided by the Gordon and Betty Moore Foundation Marine Microbiology Initiative (grant #3780) and an early career grant from the U.S. Department of Energy, Office of Biological and Environmental Research to VJO.

REFERENCES

Amann RI, Krumholz L, Stahl DA (1990) Fluorescent-oligonucleotide probing of whole cells for determinative, phylogenetic, and environmental studies in microbiology. *Journal of Bacteriology* **172**, 762–770.

Boetius A, Ravenschlag K, Schubert CJ, Rickert D, Widdel F, Gieseke A, Amann R, Jorgensen BB, Witte U, Pfannkuche O (2000) A marine microbial consortium apparently mediating anaerobic oxidation of methane. *Nature* **407**, 623–626.

Brileya KA, Camilleri LB, Zane GM, Wall JD, Fields MW (2014) Biofilm growth mode promotes maximum carrying capacity and community stability during product inhibition syntrophy. *Frontiers in Microbiology* **5**, 1–13.

Brown SD, Hurt RA Jr, Gilmour CC, Elias DA (2013) Draft genome sequences for three mercury-methylating, sulfate-reducing bacteria. *Genome Announcements* **1**, 1–2.

Campbell BJ, Li C, Sessions AL, Valentine DL (2009) Hydrogen isotopic fractionation in lipid biosynthesis by H_2-consuming *Desulfobacterium autotrophicum*. *Geochimica et Cosmochimica Acta* **73**, 2744–2757.

Caporaso JG, Kuczynski J, Stombaugh J, Bittinger K, Bushman FD, Costello EK, Fierer N, Pena AG, Goodrich JK, Gordon JI, Huttley GA, Kelley ST, Knights D, Koenig JE, Ley RE, Lozupone CA, Mcdonald D, Muegge BD, Pirrung M, Reeder J, Sevinsky JR, Turnbaugh PJ, Walters WA, Widmann J, Yatsunenko T, Zaneveld J, Knight R (2010) QIIME allows analysis of high-throughput community sequencing data. *Nature Methods* **7**, 335–336.

Coplen TB (2011) Guidelines and recommended terms for expression of stable-isotope-ratio and gas-ratio measurement results. *Rapid Communications in Mass Spectrometry* **25**, 2538–2560.

Coplen TB, Brand WA, Gehre M, Gröning M, Meijer HaJ, Toman B, Verkouteren RM (2006) After two decades a second anchor for the VPDB $\delta^{13}C$ scale. *Rapid Communications in Mass Spectrometry* **20**, 3165–3166.

Dawson KS, Schaperdoth I, Freeman KH, Macalady JL (2013) Anaerobic biodegradation of the isoprenoid biomarkers pristane and phytane. *Organic Geochemistry* **65**, 118–126.

Dirghangi SS, Pagani M (2013) Hydrogen isotope fractionation during lipid biosynthesis by *Haloarcula marismortui*. *Geochimica et Cosmochimica Acta* **119**, 381–390.

Edgar RC (2010) Search and clustering orders of magnitude faster than BLAST. *Bioinformatics* **26**, 2460–2461.

Elvert M, Boetius A, Knittel K, Jørgensen BB (2003) Characterization of specific membrane fatty acids as chemotaxonomic markers for sulfate-reducing bacteria involved in anaerobic oxidation of methane. *Geomicrobiology Journal* **20**, 403–419.

Fang J, Li C, Zhang L, Davis T, Kato C, Bartlett DH (2014) Hydrogen isotope fractionation in lipid biosynthesis by the piezophilic bacterium Moritella japonica DSK1. *Chemical Geology* **367**, 34–38.

Glass JB, Yu H, Steele JA, Dawson KS, Sun S, Chourey K, Pan C, Hettich RL, Orphan VJ (2014) Geochemical, metagenomic and metaproteomic insights into trace metal utilization by methane-oxidizing microbial consortia in sulphidic marine sediments. *Environmental Microbiology* **16**, 1592–1611.

Glöckner FO, Amann R, Alfreider A, Pernthaler J, Psenner R, Trebesius K, Schleifer K-H (1996) An in situ hybridization protocol for detection and identification of planktonic bacteria. *Systematic and Applied Microbiology* **19**, 403–406.

Goffredi SK, Wilpiszeski R, Lee R, Orphan VJ (2008) Temporal evolution of methane cycling and phylogenetic diversity of archaea in sediments from a deep-sea whale-fall in Monterey Canyon, California. *ISME Journal* **2**, 204–220.

Green-Saxena A, Dekas AE, Dalleska NF, Orphan VJ (2014) Nitrate-based niche differentiation by distinct sulfate-reducing bacteria involved in the anaerobic oxidation of methane. *ISME Journal*, **8**, 150–163.

Griffiths MJ, Van Hille RP, Harrison STL (2010) Selection of direct transesterification as the preferred method for assay of fatty acid content of microalgae. *Lipids* **45**, 1053–1060.

Hai T, Lange D, Rabus R, Steinbüchel A (2004) Polyhydroxyalkanoate (PHA) accumulation in sulfate-reducing bacteria and identification of a class III PHA synthase (PhaEC) in *Desulfococcus multivorans*. *Applied and Environmental Microbiology* **70**, 4440–4448.

Heinzelmann SM, Villanueva L, Sinke-Schoen D, Sinninghe Damsté JS, Schouten S, van der Meer MT (2015) Impact of metabolism and growth phase on the hydrogen isotopic composition of microbial fatty acids. Frontiers in Microbiology doi: 10.3389/fmicb.2015.00408 [Epub ahead of print].

Hillesland KL, Stahl DA (2010) Rapid evolution of stability and productivity at the origin of a microbial mutualism. *Proceedings of the National Academy of Sciences* **107**, 2124–2129.

Hoehler TM, Alperin MJ, Albert DB, Martens CS (1994) Field and laboratory studies of methane oxidation in an anoxic marine sediment: Evidence for a methanogen-sulfate reducer consortium. *Global Biogeochemical Cycles* **8**, 451–463.

Jendrossek D, Handrick R (2002) Microbial degradation of polyhydroxyalkanoates. *Annual Review of Microbiology* **56**, 403–432.

Jones AA, Sessions AL, Campbell BJ, Li C, Valentine DL (2008) D/H ratios of fatty acids from marine particulate organic matter in the California Borderlands Basins. *Organic Geochemistry* **39**, 485–500.

Kellermann MY, Wegener G, Elvert M, Yoshinaga MY, Lin Y-S, Holler T, Mollar XP, Knittel K, Hinrichs K-U (2012) Autotrophy as a predominant mode of carbon fixation in anaerobic methane-oxidizing microbial communities. *Proceedings of the National Academy of Sciences* **109**, 19321–19326.

Knittel K, Lösekann T, Boetius A, Kort R, Amann R (2005) Diversity and distribution of methanotrophic archaea at cold seeps. *Applied and Environmental Microbiology* **71**, 467–479.

Kotsyurbenko O (2005) Trophic interactions in the methanogenic microbial community of low-temperature terrestrial ecosystems. *FEMS Microbiology Ecology* **53**, 3–13.

Kreuzer-Martin HW, Lott MJ, Ehleringer JR, Hegg EL (2006) Metabolic processes account for the majority of the intracellular water in log-phase *Escherichia coli* cells as revealed by hydrogen isotopes. *Biochemistry* **45**, 13622–13630.

Li C, Sessions AL, Kinnaman FS, Valentine DL (2009) Hydrogren-isotopic variability in lipids from Santa Barbara Basin sediments. *Geochimica et Cosmochimica Acta* **73**, 4803–4823.

Manz W, Eisenbrecher M, Neu TR, Szewzyk U (1998) Abundance and spatial organization of gram-negative sulfate-

reducing bacteria in activated sludge investigated by in situ probing with specific 16S rRNA targeted oligonucleotides. *FEMS Microbiology Ecology* **25**, 43–61.
Matsuki T, Watanabe K, Fujimoto J, Miyamoto Y, Takada T, Matsumoto K, Oyaizu H, Tanaka R (2002) Development of 16S rRNA-gene-targeted group-specific primers for the detection and identification of predominant bacteria in human feces. *Applied and environmental microbiology* **68**, 5445–5451.
Milucka J, Ferdelman TG, Polerecky L, Franzke D, Wegener G, Schmid M, Lieberwirth I, Wagner M, Widdel F, Kuypers MMM (2012) Zero-valent sulphur is a key intermediate in marine methane oxidation. *Nature* **491**, 541–551.
Moran JJ, House CH, Vrentas JM, Freeman KH (2008) Methyl sulfide production by a novel carbon monoxide metabolism in *Methanosarcina acetivorans*. *Applied and Environmental Microbiology* **74**, 540–542.
Naraoka H, Uehara T, Hanada S, Kakegawa T (2010) δ13C–δD distribution of lipid biomarkers in a bacterial mat from a hot spring in Miyagi Prefecture, NE Japan. *Organic Geochemistry* **41**, 398–403.
Nielsen PH (1987) Biofilm dynamics and kinetics during high-rate sulfate reduction under anaerobic conditions. *Applied and Environmental Microbiology* **53**, 27–32.
Niemann H, Elvert M (2008) Diagnostic lipid biomarker and stable carbon isotope signatures of microbial communities mediating the anaerobic oxidation of methane with sulphate. *Organic Geochemistry* **39**, 1668–1677.
Oelgeschläger E, Rother M (2009) Influence of carbon monoxide on metabolite formation in *Methanosarcina acetivorans*. *FEMS Microbiology Letters* **292**, 254–260.
Orcutt B, Meile C (2008) Constraints on mechanisms and rates of anaerobic oxidation of methane by microbial consortia: process-based modeling of ANME-2 archaea and sulfate reducing bacteria interactions. *Biogeosciences Discussions*, **5**, 1933–1967.
Orphan VJ, Hinrichs K-U, Ussler W, Paull CK, Taylor LT, Sylva SP, Hayes JM, Delong EF (2001) Comparative analysis of methane-oxidizing archaea and sulfate-reducing bacteria in anoxic marine sediments. *Applied and Environmental Microbiology* **67**, 1922–1934.
Osburn MR (2013) Isotopic proxies for microbial and environmental change: insights hydrogen isotopes and the Ediacaran Khufai Formation. California Institute of Technology, Dissertation (Ph.D.).
Osburn MR, Sessions AL, Pepe-Ranney C, Spear JR (2011) Hydrogen-isotopic variability in fatty acids from Yellowston National park hot spring microbial communities. *Geochimica et Cosmochimica Acta* **75**, 4830–4845.
Pereira IaC, Ramos AR, Grein F, Marques MC, Da Silva SM, Venceslau SS (2011) A comparative genomic analysis of energy metabolism in sulfate reducing bacteria and archaea. *Frontiers in Microbiology*, **2**, 1–22.
Pernthaler A, Dekas AE, Brown CT, Goffredi SK, Embaye T, Orphan VJ (2008) Diverse syntrophic partnerships from deep-sea methane vents revealed by direct cell capture and metagenomics. *Proceedings of the National Academy of Sciences* **105**, 7052–7057.
Quast C, Pruesse E, Yilmaz P, Gerken J, Schweer T, Yarza P, Pepiles J, Glöckner FO (2013) The SILVA ribosomal RNA gene database project: improved data processing and web-based tools. *Nucleic Acids Research* **41**, D590–D596.
Raskin L, Rittmann BE, Stahl DA (1996) Competition and coexistence of sulfate-reducing and methanogenic populations in anaerobic biofilms. *Applied and Environmental Microbiology* **62**, 3847–3857.
Robins RJ, Billault I, Duan J-R, Guiet S, Pionnier S, Zhang B-L (2003) Measurement of ^{2}H distribution in natural product by quantitative ^{2}H NMR: an approach to understanding metabolism and enzyme mechanism? *Phytochemistry Reviews*, **2**, 87–102.
Rother M, Metcalf WW (2004) Anaerobic growth of *Methanosarcina acetivorans* C2A on carbon monoxide: an unusual way of life for a methanogenic archaeon. *Proceedings of the National Academy of Sciences of the United States of America* **101**, 16929–16934.
Saito K, Kawaguchi A, Okuda S, Seyama Y, Yamakawa T (1980) Incorporation of hydrogen atoms from deuterated water and stereospecifically deuterium-labeled nicotinamide nucleotides into fatty acids with the *Escherichia coli* fatty acids synthetase system. *Biochimica et Biophysica Acta* **618**, 202–213.
Sauer U, Canonaco F, Heri S, Perrenoud A, Fischer E (2004) The soluble and membrane-bound transhydrogenases UdhA and PntAB have divergent functions in NADPH metabolism of *Escherichia coli*. *Journal of Biological Chemistry* **279**, 6613–6619.
Schreiber L, Holler T, Knittel K, Meyerdierks A, Amann R (2010) Identification of the dominant sulfate-reducing bacterial partner of anaerobic methanotrophs of the ANME-2 clade. *Environmental Microbiology* **12**, 2327–2340.
Sessions AL (2006) Seasonal changes in D/H fractionation accompanying lipid biosynthesis in *Spartina alterniflora*. *Geochimica et Cosmochimica Acta* **70**, 2153–2162.
Sessions AL, Burgoyne TW, Schimmelmann A, Hayes JM (1999) Fractionation of hydrogen isotopes in lipid biosynthesis. *Organic Geochemistry* **30**, 1193–1200.
Sessions AL, Burgoyne TW, Hayes JM (2001) Correction of H_3^+ contributions in hydrogen isotope ratio monitoring mass spectrometry. *Analytical Chemistry* **73**, 192–199.
Sessions AL, Jahnke LL, Schimmelmann A, Hayes JM (2002) Hydrogen isotope fractionation in lipids of the methane-oxidizing bacterium *Methylococcus capsulatus*. *Geochimica et Cosmochimica Acta* **66**, 3955–3969.
Seyama Y, Kawaguchi A, Kusama T, Sasaki K, Arai K, Okuda S, Yamakawa T (1978) Identification of sources of hydrogen atoms in fatty acids synthesized using deuterated water and stereospecifically deuterium labeled NADPH by gas chromatographic mass spectrometric analysis. *Biomedical Mass Spectrometry* **5**, 357–361.
Sieber JR, Mcinerney MJ, Gunsalus RP (2012) Genomic insights into syntrophy: the paradigm for anaerobic metabolic cooperation. *Annual Review of Microbiology* **66**, 429–452.
Soo RM, Skennerton CT, Sekiguchi Y, Imelfort M, Paech SJ, Dennis PG, Steen JA, Parks DH, Tyson GW, Hugenholtz P (2014) Photosynthesis is not a universal feature of the phylum Cyanobacteria. *PeerJ PrePrints*, 2.
Stahl DA, Amann R (1991) Development and application of nucelic acid probes. In: *Nucleic Acid Techniques in Bacterial Systematics* (eds Stackebrandt E, Goodfellow M). John Wiley & Sons Ltd, Chichester, UK, pp. 205–248.
Stams AJM (1994) Metabolic interactions between anaerobic bacteria in methanogenic environments. *Antonie van Leeuwenhoek* **66**, 271–294.
Stams AJM, Plugge CM (2009) Electron transfer in syntrophic communities of anaerobic bacteria and archaea. *Nature Reviews Microbiology* **7**, 568–577.
Strąpoć D, Mastalerz M, Dawson K, Macalady JL, Callaghan A, Wawrik B, Ashby M (2011) Biogeochemistry of Coal-Bed Methane. *Annual Review of Earth and Planetary Sciences* **39**, 617–656.
Strous M, Jetten MSM (2004) Anaerobic oxidation of methane and ammonium. *Annual Review of Microbiology* **58**, 99–117.

Taidi B, Mansfield DA, Anderson AJ (1995) Turnover of poly(3-hydroxybutyrate) (PHB) and its influence on the molecular mass of the polymer accumulated by *Alcaligenes eutrophus* during batch culture. *FEMS Microbiology Letters* **129**, 201–205.
Thauer RK (1998) Biochemistry of methanogenesis: a tribute to marjory Stephenson: 1998 marjory Stephenson prize lecture. *Microbiology* **144**, 2377–2406.
Valentine DL (2009) Isotopic remembrance of metabolism past. *Proceedings of the National Academy of Sciences* **106**, 12565–12566.
Valentine DL, Sessions AL, Tyler SC, Chidthaisong A (2004) Hydrogen isotope fractionation during H_2/CO_2 acetogenesis: hydrogen utilization efficiency and the origin of lipid-bound hydrogen. *Geobiology* **2**, 179–188.
Wang Y, Sessions AL (2008) Memory effects in compound-specific D/H analysis by gas chromatography/pyrolysis/isotope-ratio mass spectrometry. *Analytical Chemistry* **80**, 9162–9170.
Wegener G, Niemann H, Elvert M, Hinrichs K-U, Boetius A (2008) Assimilation of methane and inorganic carbon by microbial communities mediating the anaerobic oxidation of methane. *Environmental Microbiology* **10**, 2287–2298.
Widdel F (2010) *Theory and Measurement of Bacteria*. University of Bremen, Bremen.
Widdel F, Kohring G-W, Mayer F (1983) Studies on dissimilatory sulfate-reducing bacteria that decompose fatty acids. *Archives of Microbiology* **134**, 286–294.
Zehnder AJB, Brock TD (1980) Anaerobic methane oxidation: occurence and ecology. *Applied and Environmental Microbiology* **39**, 194–204.
Zhang X, Gillespie AL, Sessions AL (2009) Large D/H variations in bacterial lipids reflect central metabolic pathways. *Proceedings of the National Academy of Sciences* **106**, 12580–12586.
Zinder SH (1993) Physiological ecology of methanogens. In *Methanogenesis*. (ed Ferry J). Springer, USA, pp. 128–206.

SUPPORTING INFORMATION

Additional Supporting Information may be found in the online version of this article:

Table S1. Fatty acid concentration (μg g^{-1}) and δD for sediment depth profiles (0–15 cm) from three characteristic methane seep habitats including sediments underlying sulfide-oxidizing microbial mats (PC18, 36, 47), chemosynthetic clam beds (PC23), and low methane flux sediment outside of visible signs of seepage (PC3).

Table S2. Archaeal and Bacterial 16S rRNA tag pyrosequencing results showing the number of sequences per taxa for genera representing greater than 1% of at least one depth horizon from sediments underlying a sulfide-oxidizing microbial mat (PC18).

Fig. S1. Partial GC-MS chromatograms for (A) *D. multivorans* and (B) the *D. multivorans/M. acetivorans* co-culture grown on benzoate indicating the four most abundant fatty acids (*ai*-$C_{15:0}$, $C_{16:0}$, *cy*-$C_{17:0}$, *me*-$C_{16:0}$) and an internal standard (I.S.).